Journal of Coordination Chemistry

ISSN: (Print) (Online) Journal homepage: www.tandfonline.com/journals/gcoo20

Substitution reactions of *cis*-platinum(II) complexes containing bidentate *N,N*-donor pyridinecarboxamide ligands with different substituents

Tshephiso R. Papo, Deogratius Jaganyi & Allen Mambanda

To cite this article: Tshephiso R. Papo, Deogratius Jaganyi & Allen Mambanda (2022) Substitution reactions of *cis*-platinum(II) complexes containing bidentate *N,N*-donor pyridinecarboxamide ligands with different substituents, Journal of Coordination Chemistry, 75:19-24, 2557-2573, DOI: 10.1080/00958972.2022.2149327

To link to this article: https://doi.org/10.1080/00958972.2022.2149327

JOURNAL OF COORDINATION CHEMISTRY
2022, VOL. 75, NOS. 19–24, 2557–2573
https://doi.org/10.1080/00958972.2022.2149327

Substitution reactions of *cis*-platinum(II) complexes containing bidentate *N,N*-donor pyridinecarboxamide ligands with different substituents

Tshephiso R. Papo[a], Deogratius Jaganyi[b,c] and Allen Mambanda[a]

[a]School of Chemistry and Physics, University of KwaZulu-Natal, Pietermaritzburg, South Africa; [b]School of Pure and Applied Sciences, Mount Kenya University, Thika, Kenya; [c]Department of Chemistry, Faculty of Applied Sciences, Durban University of Technology, Durban, South Africa

ABSTRACT

Substitution reactions of [2-(pyridinecarboxamide)dichloride Pt(II)] [**$PtCl_2$**], [*N*-phenyl-(2-pyridinecarboxamide)dichloride Pt(II)] [**$PhPtCl_2$**], [*N*-(4-methylphenyl)-2-pyridinecarboxamide)dichloride Pt(II)] [**$CH_3PhPtCl_2$**], [*N*-(4-methoxyphenyl)-(2-pyridine-carboxamide)dichloride Pt(II)] [**$CH_3OPhPtCl_2$**] and [*N*-(4-fluorophenyl)-(2-pyridinecarboxamide)dichloride Pt(II)] [**$FPhPtCl_2$**], with nucleophiles; thiourea (**TU**), *N,N′*-dimethylthiourea (**DMTU**) and *N,N,N′,N′*-tetramethylthiourea (**TMTU**) were studied under *pseudo* first-order conditions. The rates of substitution were investigated as a function of nucleophile concentration and temperature using stopped-flow and UV-visible absorption spectrophotometers. Substitutions of the two coordinated chloride ligands of the Pt(II) complexes occur consecutively, with the first substitution occurring opposite the coordinated pyridyl. The observed *pseudo* first-order rate constants regressed linearly with concentration of the incoming nucleophiles according to the equation $k_{obs} = k_2[Nu]$. The highest substitution rates were measured for $PtCl_2$, which is attributed to the unsubstituted non-leaving carboxamide ligand. The Pt(II) center of this complex is the most electrophilic as a result of the strong withdrawal of electron density through π-resonance by the carboxamide group. The introduction of a 4′-substituted phenyl group on the amido *N* of the carboxamide reduces the reactivity of the complexes due to proportional electronic effects from the ancillary substituents on the phenyl ring as well as its conformational disposition with respect to the plane of the complex. The order of reactivity of studied nucleophiles is **TU** > **DMTU** > **TMTU**. The substitution is associatively activated as supported by the negative entropy of activation values for the reactions.

ARTICLE HISTORY
Received 25 August 2022
Accepted 27 October 2022

KEYWORDS
N-(4-substituted-phenyl)-(2-pyridine-carboxamide); pyridine carboxamide; Pt(II) complexes; ligand substitution; consecutive reactions

CONTACT Tshephiso R. Papo papot@ukzn.ac.za School of Chemistry and Physics, University of KwaZulu-Natal, Pietermaritzburg, South Africa

Supplemental data for this article can be accessed online at https://doi.org/10.1080/00958972.2022.2149327

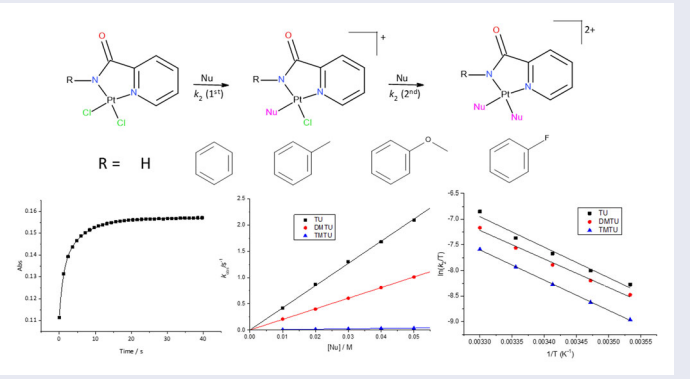

Introduction

Covalent binding to DNA by *cis* square-planar Pt(II) compounds, in particular cisplatin and its analogues is generally accepted as the main mechanism responsible for their anticancer activity, induced by the DNA metallocycles that are formed between the *cis*-PtL_2 (non-leaving ammine) fragments and neighboring DNA bases within a strand [1, 2]. However, Pt(II) complexes can also interact with sulfur-containing bio-molecules such as the thiol-proteins and enzymes on their way to their cytotoxic target [3]. The latter phenomenon causes drug toxicity.

Alteration of the structure of the non-leaving ligand of the *cis*-PtL_2 motif has a direct influence on the binding reactivity of the complexes with DNA as well as subsequent induction of cellular damage and downstream apoptotic processes [4]. Introducing aromatic planar non-leaving ligands with substituents of variable σ-donor/π-acceptor capacity can result in favorable non-covalent interactions of the complexes with the purine/pyrimidine bases of DNA [5, 6]. Foremost is the fact that the rate at which that occurs can be tuned by attaching substituents of variable σ-donor/π-acceptability [6].

Substitution reactions of Pt(II) complexes with pyridine ligands have been investigated due to their potential as anticancer agents [7–9]. However, not as much reactivity data on substitution of Pt(II) complexes with the carboxamide (–CONH–) group have been reported. The carboxamide group is the primary linkage structure of amino acids and proteins. It is an important motif of the *N*-(substituted)(2-pyridyl)carboxamide, a bidentate non-leaving ligand with potential to bring synergistic effects in the *cis*-PtL_2 coordination geometry. Previous studies on DNA binding properties of the *N*-substituted pyridine carboxamide ligands indicate that the ligands bind to DNA *via* intercalation [10–12]. This ligand has diverse structural chemistry and forms complexes similar to metal peptides [13] that have potential to meet target specificity for nucleic sites such as DNA [14, 15].

Pyridine-carboxamide is derived from picolinic acid which is an isomer of nicotinic acid. The latter is the body's prime natural chelator of vital trace elements such as chromium, zinc, copper, manganese, iron, copper and molybdenum [16]. Picolinic acid

is biosynthesized in the liver and kidneys from the amino acid tryptophan [16]. It is stored in the pancreas and secreted into the intestine during digestion. Pt(II) complexes containing picolinic acid derived from a pyridine carboxamide have been synthesized and demonstrated to have notable activity against human and murine leukemia cells [17].

Reactivity data on the nucleophilic interactions of Pt(II) complexes with sulfur-containing biomolecules are crucial in informing new strategies for the future development of platinum-based anticancer agents of improved efficacy compared to existing drugs. A combination of strength of the σ-donor groups as well as π-acceptor capabilities of the pyridine-bearing non-leaving ligands of monofunctional Pt(II) complexes control the rate at which co-ligands are substituted, be it in opposite ways [18–20]. Corroborating this were two studies on the reactivity of Pt(II) complexes with pyridyl/quinolinyl-pyrazole/thioether bidentate ligands [21–25]. Electron-donating groups on the 3,5 positions of a coordinated pyridyl/quinolinyl-pyrazole ring of the bidentate ligands decreased the rate of substitution [21–26]. Electron-withdrawing groups at the same positions increased the rate of reaction by withdrawing electron density from the pyrazole ring, thereby switching it from a net σ-donor to a π-acceptor [21, 25].

In the present study, we report on the substitution reactions of *cis*-[-(4-substituted-phenyl)-(2-pyridine-carboxamide)Pt(II)Cl_2] complexes with sulfur-containing nucleophiles. The five complexes have bidentate ligands with a common pyridyl-N donor and amide-N donor with different substituents, *viz*. NH_2, phenyl, phenyl–CH_3, phenyl–OCH_3 and phenyl–F. The bidentate *N*-donor confers thermodynamic stability to the complexes through the chelate effect. The structures of the ligands have a common geometry to the anticancer drug cisplatin and its analogues.

Materials and instrumentation

The following chemicals and reagents, picolinamide, 2-picolinic acid, aniline, 4-methyl-aniline, 4-fluoro-aniline, p-anisidine, triphenylphosphite, potassium tetrachloroplatinate, thiourea, *N,N′*-dimethylthiourea and *N,N,N′,N′*-tetramethylthiourea were purchased from Sigma-Aldrich and used without purification. All solvents were procured from Merck South Africa and were of analytical grade.

Bruker Avance III 400 or Bruker Avance III 500 spectrometers were used to record ^{1}H and ^{195}Pt NMR spectra at 400 MHz or 500 MHz using either a 5 mm BBOZ probe or a 5 mm TBIZ probe. Chemical shifts for all protons are quoted relative to the relevant solvent signal. All data were recorded at 303 K. The mass spectrometric data of the ligands and platinum complexes were attained on a Waters Micromass LCT Premier mass spectrometer. Elemental compositions were obtained on a Carlo Erba Elemental Analyzer 1.106.

A Varian Cary 100 Bio UV-visible spectrophotometer was used to determine the wavelengths for kinetic studies. Kinetic measurements were carried out on an Applied Photophysics SX.18 MV (v4.33) stopped-flow analyzer coupled to an online data acquisition system. The temperature was controlled throughout all kinetic experiments to within ±0.1 °C using a coupled temperature control unit. All data were analyzed using the Origin 9.1® (OriginLab Corporation, Northampton, MA) graphical analysis software package.

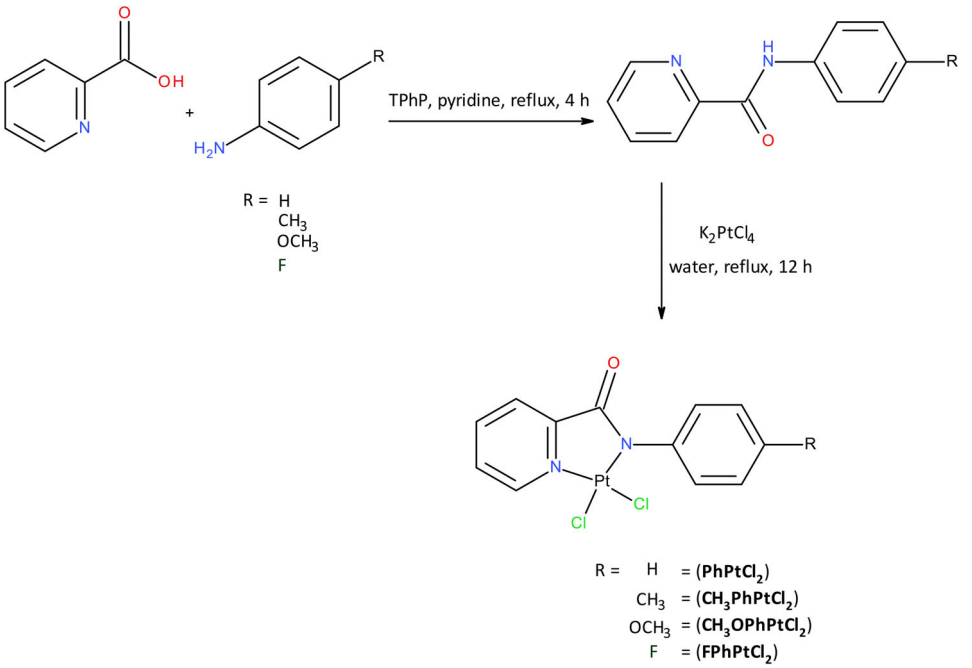

Scheme 1. Synthetic pathway for the ligands and their respective Pt(II) complexes.

Synthesis and characterization of the ligands

The ligands, *N*-(phenyl)-pyridine-2-carboxamide, *N*-(4-methylphenyl)-pyridine-2-carboxamide, *N*-(4-methoxyphenyl)-pyridine-2-carboxamide and *N*-(4-fluorophenyl)-pyridine-2-carboxamide were synthesized following a reported method [27] with slight modifications (Scheme 1).

Solutions of 2-picolinic acid (5 mmol) and of the corresponding anilines (aniline, 4-methylaniline, 4-fluoro-aniline, p-anisidine) (5 mmol) in pyridine (8 mL) were mixed under stirring at 100 °C followed by the dropwise addition of triphenylphosphite (5 mmol). The mixture was further stirred for 4 h at 100 °C then cooled to room temperature, and the desired products isolated as described hereafter.

N-phenyl-pyridine-2-carboxamide: The cooled solution was concentrated and an off-white precipitate was formed and washed with diethyl ether. Yield: 73%. ^{1}H NMR (400 MHz, $CDCl_3$, 303.15 K) [δ, ppm]: 10.01 (s, 1H); 8.62 (s, 1H); 8.29 (d, 1H); 7.91 (t, 1H); 7.74 (m, 2H); 7.49 (m, 1H); 7.16 (m, 1H); 7.08 (d, 2H). ^{13}C NMR (400 MHz, $CDCl_3$, 303.15 K) [δ, ppm]: 161.69; 149.67; 147.64; 138.05; 137.74; 129.08; 126.52; 124.39; 122.70; 119.77. TOF MS ESI^{+}: *m/z* 221 (calculated *m/z* 198.22), [$(M + Na)^{+}$].

N-(4-methylphenyl)-pyridine-2-carboxamide: Water was added to the solution to induce formation of a white solid. The solid was collected by filtration and washed with diethyl ether to get a pure white product. Yield: 58%. ^{1}H NMR (400 MHz, $CDCl_3$, 303.15 K) [δ, ppm]: 9.82 (s, 1H); 8.73 (d, 1H); 8.14 (dd, 2H); 7.61 (dd, 1H); 7.19 (dd, 2H); 7.01 (m, 2H); 2.95 (s, 3H). ^{13}C NMR (400 MHz, $CDCl_3$, 303.15 K) [δ, ppm]: 161.54; 149.42; 147.46; 138.02; 136.76; 129.46; 125.43; 123.32; 121.98; 118.34; 48.98. TOF MS ESI^{+}: *m/z* 235 (calculated *m/z* 212.25), [$(M + Na)^{+}$].

N-(4-methoxyphenyl)-pyridine-2-carboxamide: On cooling the solution, a brown precipitate that formed was collected and washed with diethyl ether (8 mL). The product was redissolved in dichloromethane (5 mL). Thereafter, it was precipitated with cold hexane (5 mL), filtered and washed with cold hexane to obtain a white solid after filtration and drying. Yield: 85%. ^{1}H NMR (400 MHz, $CDCl_3$, 303.15 K) [δ, ppm]: 9.91 (s, 1H); 8.61 (d, 1H); 8.30 (d, 1H); 7.91 (t, 1H); 7.69 (t, 2H); 7.47 (m, 1H); 6.93 (2H, d); 3.82 (3H, s). ^{13}C NMR (400 MHz, $CDCl_3$, 303.15 K) [δ, ppm]: 161.50; 156.45; 149.86; 147.69; 137.89; 131.04; 126.34; 122.51; 121.29; 114.26; 55.50. TOF MS ESI$^+$: *m/z* 479 (calculated *m/z* 228.25), [$(2M + Na)^+$].

N-(4-fluorophenyl)-pyridine-2-carboxamide: On cooling the solution, a white precipitate formed. It was filtered and washed with cold diethyl ether and dried thereafter. Yield: 62%. ^{1}H NMR (400 MHz, $CDCl_3$, 303.15 K) [δ, ppm]: 9.91 (s, 1H); 8.60 (d, 1H); 8.29 (d, 1H); 7.90 (t, 1H); 7.69 (m, 2H); 7.47 (m, 1H); 6.92 (2H, t). ^{13}C NMR (400 MHz, $CDCl_3$, 303.15 K) [δ, ppm]: 162.00; 149.48; 147.99; 137.73; 136.87; 132.00; 126.61; 122.61; 121.21; 116.80. TOF MS ESI$^+$: *m/z* 239 (calculated *m/z* 216.21), [$(M + Na)^+$].

Synthesis and characterization of the Pt(II) complexes

The complexes, [2-(pyridinecarboxamide)dichloride Pt(II)] [**$PtCl_2$**], [*N*-phenyl-(2-pyridinecarboxamide)dichloride Pt(II)] [**$PhPtCl_2$**], [*N*-(4-methylphenyl)-2-pyridinecarboxamide)-dichloride Pt(II)] [**$CH_3PhPtCl_2$**], [*N*-(4-methoxyphenyl)-(2-pyridine-carboxamide)dichloride Pt(II)] [**$CH_3OPhPtCl_2$**] and [*N*-(4-fluorophenyl)-(2-pyridinecarboxamide) dichloride Pt(II)] [**$FPhPtCl_2$**], were synthesized according to a literature method with minor modifications [28]. An aqueous solution of potassium tetrachloroplatinate (0.51 mmol, 3 mL) was added dropwise to a solution of the *N,N*-chelate ligand (0.5 mmol) in water (3 mL). The mixture was stirred under reflux for 4 h and thereafter allowed to cool to room temperature. The precipitate that formed was collected through 0.45 μm Millipore nylon filter paper. All complexes synthesized were subjected to analysis to determine their purity and were characterized using NMR (^{1}H and ^{195}Pt), FT-IR, CHN elemental analysis and TOF MS-ESI$^+$.

$PtCl_2$: ^{1}H NMR (400 MHz, $CDCl_3$, 303.15 K) [δ, ppm]: 8.61 (d, 1H); 8.24 (d, 1H); 7.88 (t, 1H); 7.47 (t, 1H). ^{195}Pt NMR (500 MHz; $CDCl_3$, 303.15 K) [δ, ppm] − 2225.48. TOF MS ESI$^+$: *m/z* 410.06 (calculated *m/z* 388.12), [$(M + Na)^+$]. Anal. % Calculated for $C_6H_5Cl_2N_2OPt$: C: 18.62, H: 1.30, N: 7.23. Found: C: 18.61, H: 1.38, N: 7.25.

[**$PhPtCl_2$**]: ^{1}H NMR (400 MHz, DMSO-d_6, 303.15 K) [δ, ppm]: 7.89 (s, 1H); 7.62 (dd, 1H); 7.41 (dd, 2H); 7.22 (d, 2H); 7.19 (d, 2H); 6.97 (dd, 1H). ^{195}Pt NMR (500 MHz; DMF-d_7, 303.15 K) [δ, ppm] − 2275.56. TOF MS ESI$^+$: *m/z* 485.91 (calculated *m/z* 463.2026), [$(M + Na)^+$]. Anal. % Calculated for $C_{12}H_9Cl_2N_2OPt$: C: 31.11, H: 1.96, N: 6.05. Found: C: 31.26, H: 2.01, N: 6.21.

[**$CH_3PhPtCl_2$**]: ^{1}H NMR (400 MHz, DMSO-d_6, 303.15 K) [δ, ppm]: 8.98 (d, 1H); 8.35 (dd, 2H); 7.87 (dd, 1H); 7.32 (dd, 2H); 7.32 (m, 2H); 3.02 (s, 3H). ^{195}Pt NMR (500 MHz; DMF-d_7, 303.15 K) [δ, ppm] − 2288.32. TOF MS ESI$^+$: *m/z* 500.25 (calculated *m/z* 477.2292), [$(M + Na)^+$]. Anal. % Calculated for $C_{13}H_{11}Cl_2N_2OPt$: C: 32.71, H: 2.32, N: 5.87. Found: C: 33.01, H: 2.45, N: 5.92.

[**$CH_3OPhPtCl_2$**]: ^{1}H NMR (400 MHz, $CDCl_3$, 303.15 K) [δ, ppm]: 8.66 (d, 1H); 8.28 (d, 1H); 7.98 (t, 1H); 7.63 (t, 1H); 7.01 (d, 2H); 6.84 (2H, d); 3.78 (3H, s). ^{195}Pt NMR

(500 MHz; $CDCl_3$, 303.15 K) [δ, ppm] − 2542.16. TOF MS ESI^+: *m/z* 516.24 (calculated *m/z* 493.2286), $[(M + Na)^+]$. Anal. % Calculated for $C_{13}H_{11}Cl_2N_2O_2Pt$: C: 31.65, H: 2.65, N: 5.68. Found: C: 31.62, H: 2.26, N: 5.62.

[**FPhPtCl$_2$**]: ^{1}H NMR (400 MHz, DMSO-d_6, 303.15 K) [δ, ppm]: 8.99 (d, 1H); 8.49 (d, 1H); 8.30 (t, 1H); 8.08 (m, 2H); 7.88 (m, 1H); 7.42 (2H, t). ^{195}Pt NMR (500 MHz; DMF-d_7, 303.15 K) [δ, ppm] − 2486.51. TOF MS ESI^+: *m/z* 504.07 (calculated *m/z* 481.193), $[(M + Na)^+]$. Anal. % Calculated for $C_{12}H_8Cl_2FN_2OPt$: C: 29.95, H: 1.67, N: 5.82. Found: C: 29.92, H: 1.66, N: 5.78.

Results

Synthesis of ligands and Pt(II) complexes

The ligands were synthesized from the reaction of 2-picolinic acid and *N*-substituted amines in the presence of triphenylphosphite to produce the corresponding *N*-substituted amines in excellent yield. Treatment of ligands (picolinamide, *N*-phenylpyridine-2-carboxamide, *N*-(4-methylphenyl)-pyridine-2-carboxamide, *N*-(4-methoxyphenyl)-pyridine-2-carboxamide and *N*-(4-fluorophenyl)-pyridine-2-carboxamide) with aqueous potassium tetrachloroplatinate (K_2PtCl_4) produced the corresponding Pt(II) complexes in moderate yields (Scheme 1). The ligands and their Pt(II) complexes were characterized using ^{1}H and ^{195}Pt NMR, FT-IR spectroscopy, mass spectrometry and elemental analysis.

^{1}H NMR spectra of the ligands and the corresponding Pt(II) complexes show the expected peak multiplicities and integrations (ESI). The ^{1}H NMR spectra of the Pt(II) complexes show that the pyridyl protons are deshielded compared to the free ligands, which proves that the ligand coordinated to the metal ion. The identity of Pt(II) complexes was further confirmed by comparing their FT-IR spectra to their corresponding ligands (Supplementary Figures S14–S17). For example, the amidic N − H band of *N*-(4-methoxyphenyl)-pyridine-2-carboxamide was at 3355 cm^{-1} and is absent in the spectrum of the respective Pt(II) complex (**CH$_3$OPhPtCl$_2$**), confirming the N − H deprotonated upon complexation. The infrared spectra of the complexes illustrate that the absorption frequencies for the C = O group are almost unshifted as compared to those observed in free ligands. This observation clearly indicates that the C = O group is uncoordinated to Pt(II) in all complexes.

Elemental analysis data of the complexes were consistent with the proposed structures in Scheme 1 and confirmed the stoichiometric ratios and purity of the complexes.

Density functional theory calculations

In order to get data to explain the observed kinetic trend due to the influence of changing substituents on the structural and electronic properties of the *cis*-Pt(II) complexes, computational calculations were performed. The Pt(II) dichloro complexes were optimized to identify energy-minimized ground state structures in the gaseous phase using the B3LYP/LanL2DZ basis set [29–32]. The structures were optimized by density functional theory (DFT) using Gaussian 09 suite of programs [33]. The singlet states were used due to low electronic spin of Pt(II) complexes. From the ground-state

Table 1. DFT-Calculated HOMO and LUMO frontier molecular orbitals of Pt(II) complexes.

Geometry optimized	HOMO map	LUMO map	Planarity
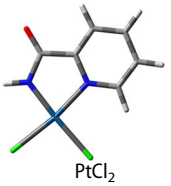 $PtCl_2$	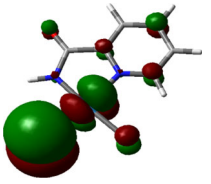	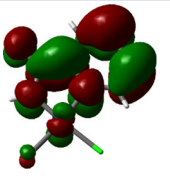	
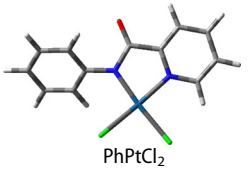 $PhPtCl_2$	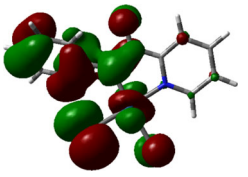	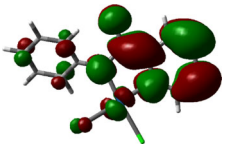	
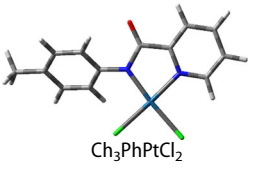 $Ch_3PhPtCl_2$	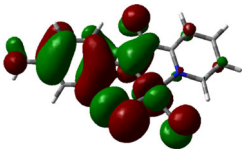	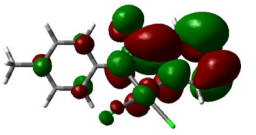	
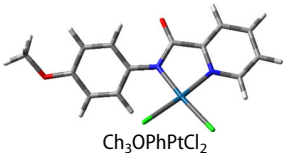 $Ch_3OPhPtCl_2$	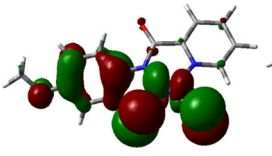	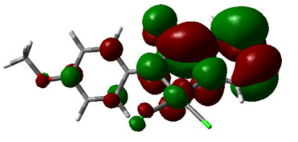	
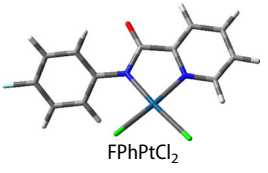 $FPhPtCl_2$	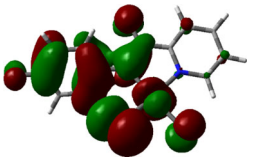	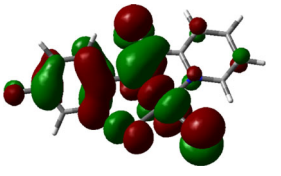	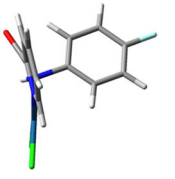

optimized electronic structures, surface potential mappings of the HOMO and LUMO were identified as shown in Table 1.

The electronic character of the ancillary substituent on phenyl ring bonded to the amido *N*-donor atom of the non-leaving ligand influences the energy difference between the HOMO and LUMO orbitals. The calculated HOMO-LUMO energy gap and significant geometrical data are summarized in Figure 1 and Table 2, respectively. DFT calculated frontier orbitals indicated in Table 1 demonstrate that the electron density of the HOMO orbitals lies mostly on the Pt(II) center, the chloride ligands and the phenyl substituents; while the LUMO electron density is largely located on the picolinamide ligand framework.

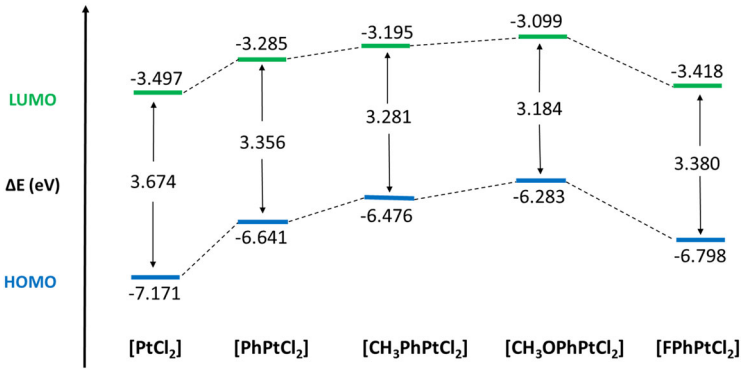

Figure 1. Calculated energies of the HOMO, LUMO and the energy gap (ΔE) of the Pt(II) complexes.

Table 2. Summary of DFT calculated data for investigated complexes.

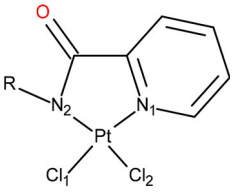

R =	H		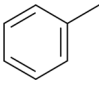	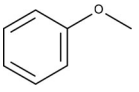	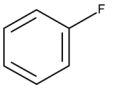
Parameter	[$PtCl_2$]	[$PhPtCl_2$]	[$PhCH_3PtCl_2$]	[$PhOCH_3PtCl_2$]	[$PhFPtCl_2$]
Bond lengths (Å)					
Pt–Cl_1	2.386	2.394	2.395	2.397	2.394
Pt–Cl_2	2.375	2.391	2.393	2.396	2.388
Pt–$N_{1(py)}$	2.076	2.055	2.051	2.048	2.055
Pt–N_2	1.936	2 .002	2.008	2.016	2.001
Bond angles (°)					
N_1-Pt-N_2	81.09	81.97	81.92	81.82	81.96
NBO charges					
Pt	0.531	0.453	0.449	0.433	0.464
Cl_1	−0.338	−0.327	−0.333	−0.345	−0.327
Cl_2	−0.277	−0.329	−0.340	−0.349	−0.320
N_1	−0.488	−0.478	−0.477	−0.476	−0.478
N_2	−0.608	−0.538	−0.540	−0.546	−0.542
O	−0.554	−0.566	−0.572	−0.583	−0.567
μ (chemical potential)	−5.334	−4.963	−4.836	−4.691	−5.108
ω (electrophilicity index)	7.74	7.34	7.13	6.91	7.72

Kinetic measurements

Substitutions of the coordinated chloride ligands from five Pt(II) complexes by three thiourea nucleophiles were studied as a function of concentration of the nucleophiles and temperature of the reaction medium. The concentration of the nucleophiles was kept at least 20-fold greater than that of the Pt(II) complexes to ensure *pseudo* first order kinetic conditions. The ionic strength of the reaction media was maintained at

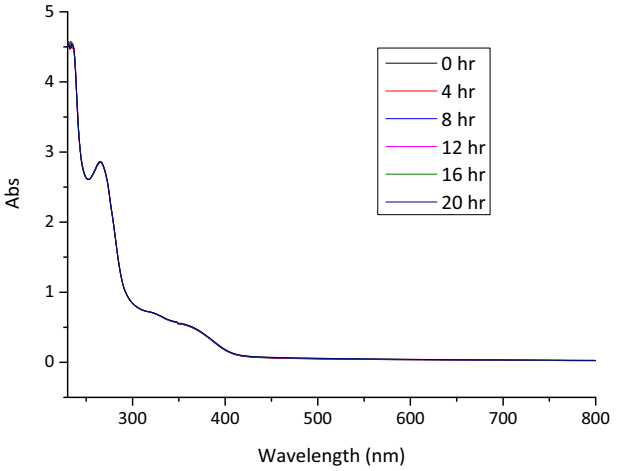

Figure 2. UV-visible scans of $\mathbf{PtCl_2}$ in 0.1 M methanol over a 20-h period.

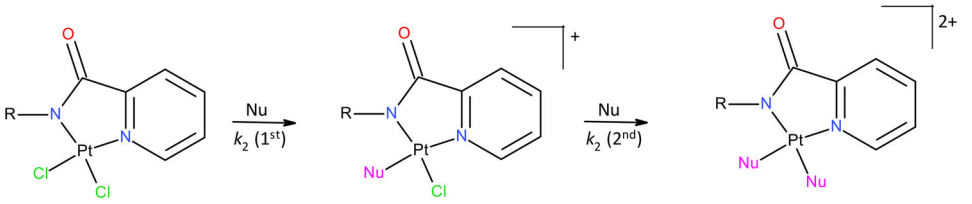

Scheme 2. Proposed reaction scheme for the substitution reaction of the studied Pt(II) complexes with thiourea nucleophiles in 0.10 M methanol solution.

0.10 M with sodium perchlorate (0.09 M) and lithium chloride (0.01 M) in methanol. The complexes were dissolved in 0.10 M methanol solution. The solvolysis stability of the complexes in methanol was established by monitoring spectral changes of their solutions over a 20-h period using the UV-visible spectrophotometer. Figure 2 shows the spectral changes for $\mathbf{PtCl_2}$; the complex is stable over the time period since no changes in absorbance are observed.

Preliminary studies were performed on the UV-visible spectrophotometer to determine suitable wavelengths for kinetic measurements. Spectral changes resulting from mixing of the Pt(II) complexes and nucleophile solutions were recorded from 200 to 800 nm. The selected wavelengths are summarized in the Supporting Information (Supplementary Table S1).

The substitution of the chloride ligands by the three nucleophiles took place *via* two consecutive reaction steps as shown in Scheme 2.

To confirm that the two substitution steps were due to the stepwise displacement of the two chloride groups as shown in Scheme 1, the substitution reaction of $\mathbf{PhPtCl_2}$ with two equivalents of **TU** was monitored by ^{195}Pt NMR spectroscopy at 303 K over 18 h. ^{195}Pt NMR spectroscopy is an effective technique for determination of the coordination details of platinum complexes. Figure 3 presents the evolution of the ^{195}Pt NMR spectra during the substitution reaction.

The initial ^{195}Pt NMR peak at −2275 ppm corresponds to unreacted $\mathbf{PhPtCl_2}$ complex. Two new peaks appear at −2812 and −3445 ppm after 20 min, the two new

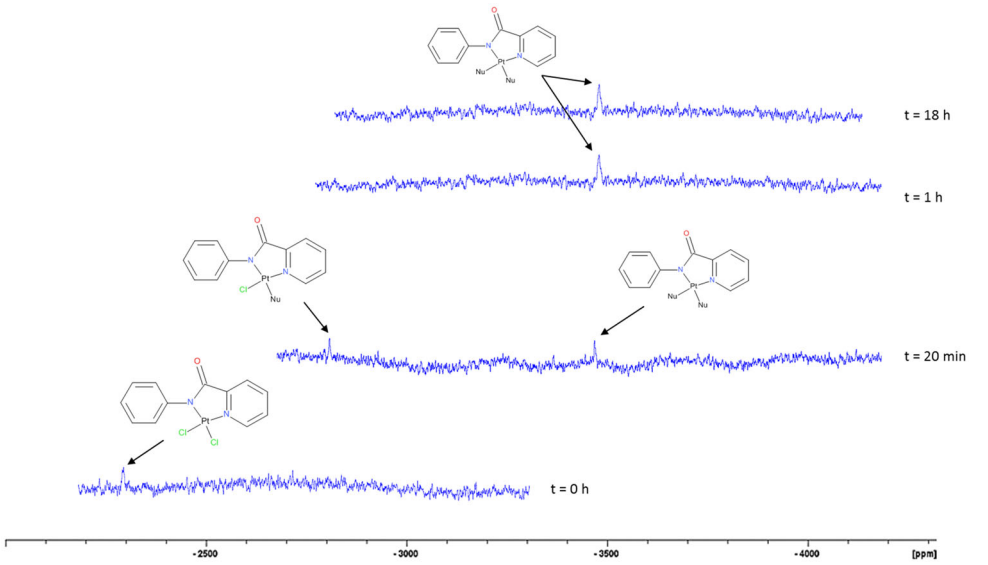

Figure 3. ^{195}Pt NMR spectra for the reaction of **PhPtCl$_2$** and two equivalents of **TU** in DMF-d_7 at 303 K over an 18-h period.

peaks are due to the formation of **PhPtN$_2$NuCl** (-2812) and **PhPtN$_2$Nu$_2$** (-3445) species (N_2=*N,N*-bidendate ligand and Nu = thiourea) *via* consecutive substitution of the first and second chloride ligands, respectively. Formation of **PhPtN$_2$NuCl** is fast and so is its subsequent reaction with a second **TU** molecule (a 50% conversion attained within 20 min) to form **PtN$_2$TU$_2$**. Within an hour, the −2812 ppm peak had completely disappeared while the peak at −3445 ppm remained constant, indicating that the ligand did not subsequently de-coordinate from the Pt(II), supported by the absence of a peak between −3800 to −4000 ppm for the [PtS_4] coordination sphere [34]. This observation supports the proposed reaction pathway given in Scheme 2. The same observation was observed for **PtCl$_2$** (Supplementary Figure S18).

All chloride substitution reactions were monitored on the stopped-flow spectrophotometer. An exception was for the second substitution step involving **CH$_3$PhPtCl$_2$** and **CH$_3$OPhPtCl$_2$**, which were monitored on the UV-visible spectrophotometer. A typical time dependent stopped-flow kinetic trace for the first chloride substitution from **FPhPtCl$_2$** by **DMTU** is shown in Figure 4.

The kinetic traces of the chloride substitution reactions for the Pt(II) complexes gave excellent fits to a single exponential function, giving the *pseudo* first order rate constants, $k_{obs(1st)}$ and $k_{obs(2nd)}$, at specific nucleophile concentration for the first and second substitution steps, respectively, according to Equation (1) [35].

$$A_t = A_o + (A_o - A_\infty) \exp(-k_{obs} t) \quad (1)$$

All the observed rate constants ($k_{obs(1st/2nd)}$ are averages of five independent kinetic runs while they were averages of duplicates for reactions of **CH$_3$PhPtCl$_2$** and **CH$_3$OPhPtCl$_2$** which were recorded on the UV-visible absorption spectrophotometer.

The *pseudo* first order rate constants, ($k_{obs(1st/2nd)}$), calculated from the kinetic traces were plotted against the concentration of the incoming nucleophile. Representative

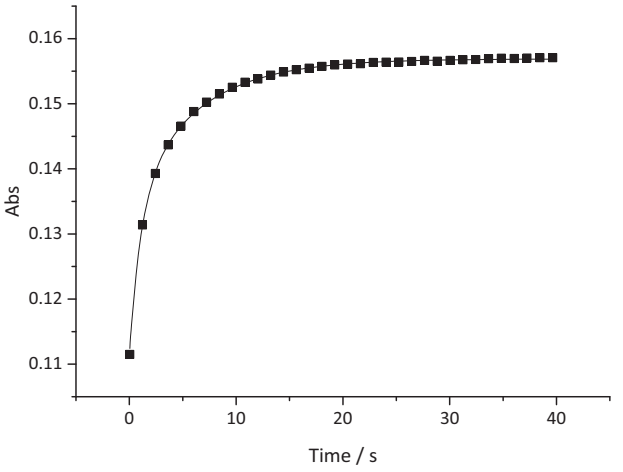

Figure 4. Stopped-flow kinetic trace at 286 nm for the first chloride substitution of **FPhPtCl$_2$** (0.5 mM) by **DMTU** (30 mM) at 298 K in a 0.10 M solution of methanol.

plots are shown in Figure 5. Straight lines with zero intercepts were obtained for each of the nucleophiles for the two substitution steps, suggesting that the mechanism of the substitution and the rate law can be represented by Equations (2) and (3). The second order rate constants were calculated from the slopes of plots of $k_{obs(1st/2nd)}$ against nucleophile concentration. These values are summarized in Table 3.

$$k_{obs}(1st) = k_2(1st)[Nu] \quad (2)$$

$$k_{obs}(2nd) = k_2(2nd)[Nu] \quad (3)$$

The effect of temperature on the rate of substitution was studied by varying the temperature of the reaction medium from 283 to 303 K. The enthalpy ($\Delta H^{\#}$) and entropy ($\Delta S^{\#}$) of activation were calculated from the slopes and y-intercepts of the Eyring plots, respectively, according to Equation (4) [35]. Representative Eyring plots are presented in Figure 6. The values of $\Delta H^{\#}$ and $\Delta S^{\#}$ are summarized in Table 4.

$$\ln\left(\frac{k_{expt}}{T}\right) = \frac{-\Delta H^{\neq}}{R}\cdot\frac{1}{T} + \left[23.8 + \frac{\Delta S^{\neq}}{R}\right] \quad (4)$$

Discussion

Substitution reactions of Pt(II) complexes with *N*-(4-substituted-phenyl)-(2-pyridine-carboxamide) bidentate ligands were investigated with three sulfur donor nucleophiles. The substitution reactions of the complexes with **TU**, **DMTU** and **TMTU** occurred in two consecutive steps (Scheme 2). Each step represents the substitution of one chloride ligand as confirmed by ^{195}Pt NMR studies in Figure 3 for the reaction of **PhPtCl$_2$** with two equivalents of **TU**. The values of the chemical shift for the product of the first chloride substitution, [PtN$_2$SCl], fall within the range −2750 to −3150 ppm, while those for the final product [PtN$_2$S$_2$] fall within −3150 to −3550 ppm [28]. Two new peaks appear at −2812 and −3445 during consecutive substitution of the chloride.

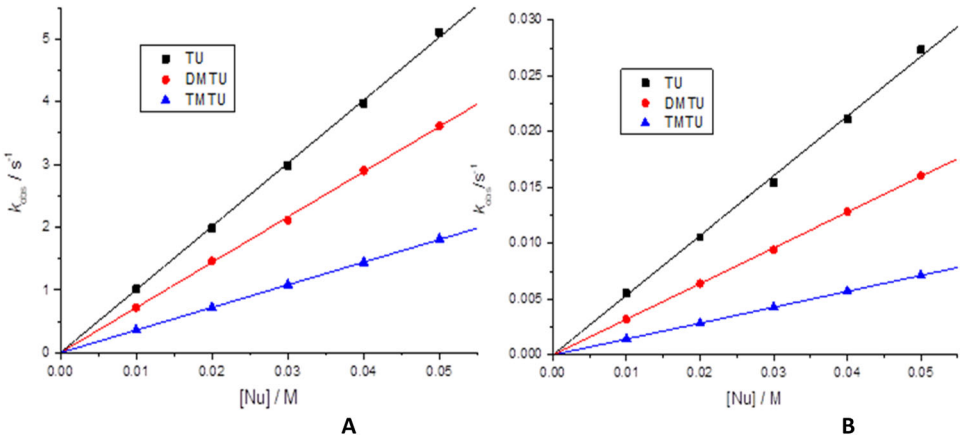

Figure 5. Dependence of the *pseudo* first-order rate constant on the concentration of thiourea nucleophiles for chloride substitution from **$CH_3OPhPtCl$** (1st substitution step (A) and 2nd substitution step (B)) in 0.1 M methanol at 298 K.

Table 3. Summary of rate constants for the substitution of chloride from the complexes by **TU**, **DMTU** and **TMTU** in 0.1 M methanol.

Complex	Nu	k_2 (1st)/M^{-1} s^{-1}	k_2 (2nd)/M^{-1} s^{-1}
$PtCl_2$	**TU**	347 ± 8	81 ± 2
	DMTU	285 ± 6	34 ± 1
	TMTU	156 ± 4	15.4 ± 0.09
$PhPtCl_2$	**TU**	129 ± 1	26.1 ± 0.3
	DMTU	41.0 ± 0.3	10.34 ± 0.02
	TMTU	9.2 ± 0.2	1.00 ± (5.2 × 10^{-3})
$CH_3PhPtCl_2$	**TU**	39.1 ± 0.6	0.39 ± (3.78 × 10^{-5})
	DMTU	17.4 ± 0.2	0.20 ± (1.9 × 10^{-4})
	TMTU	2.9 ± 0.1	(6.22 ± 0.15) × 10^{-2}
$CH_3OPhPtCl_2$	**TU**	53 ± 1	0.54 ± (6.12 × 10^{-3})
	DMTU	45.6 ± 0.5	0.32 ± (1.11 × 10^{-3})
	TMTU	8.2 ± 0.1	0.14 ± (3.41 × 10^{-5})
$FPhPtCl_2$	**TU**	212 ± 4	32.3 ± 0.3
	DMTU	183 ± 2	9.86 ± 0.02
	TMTU	33.0 ± 0.20	2.1 ± 0.1

This indicates formation of new products in solution, **PtN_2TUCl** (-2812) and **PtN_2TU_2** (-3445), formed by substitution of the first and second chloride ligands, respectively. The peak for the final substitution product was found at −3451 ppm, which confirms that the ligand remains coordinated to the metal center during the substitution of the two chloride ligands.

The rate of chloride substitution from the complexes for both steps followed the order **$PtCl_2$** > **$FPhPtCl_2$** > **$PhPtCl_2$** > **$CH_3OPhPtCl_2$** > **$CH_3PhPtCl_2$** with all the nucleophiles studied. The trend indicates that the rate of substitution from the Pt(II) complexes is influenced by the substituents attached to the phenyl group of the *N*-(4′-substituted phenyl)pyridylcarboxamide ligand. The two chloride groups are substituted at different rates due to the difference in the strength of the *trans* effect of the pyridine (py) relative to that of the amido group. This difference in *trans* effect is strongly supported by the trends in DFT data in Table 2. The natural bond orbital (NBO)

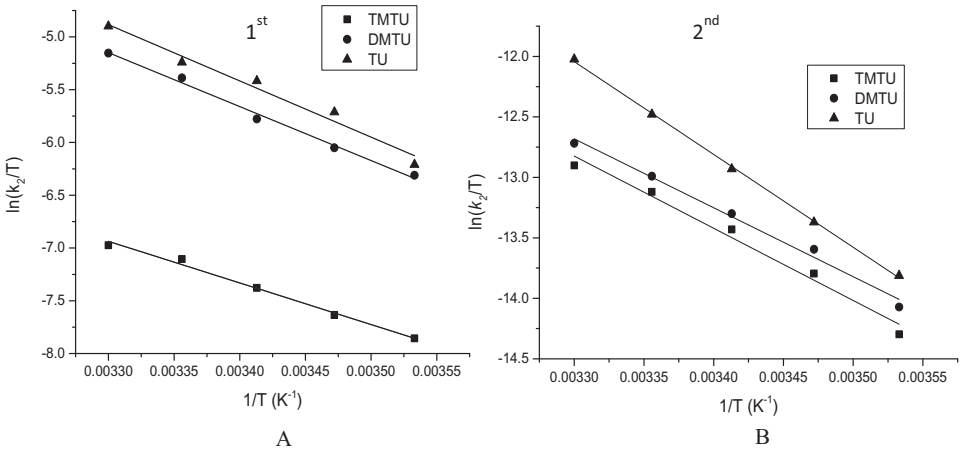

Figure 6. Eyring plots for the reactions of **$PtCl_2$** with thiourea nucleophiles for the 1st (A) and 2nd (B) substitution steps from 283 to 303 K.

Table 4. Summary of activation parameters for the substitution of chloride by **TU**, **DMTU** and **TMTU** in 0.1 M methanol.

		Activation enthalpy (kJ mol^{-1})		Activation entropy (J K^{-1} mol^{-1})	
Complex	Nu	ΔH_1	ΔH_2	ΔS_1	ΔS_2
$PtCl_2$	**TU**	44 ± 1	38 ± 5	−88 ± 3	−92 ± 14
	DMTU	43 ± 2	37 ± 3	−100 ± 6	−153 ± 9
	TMTU	33 ± 2	26 ± 2	−147 ± 5	−173 ± 5
$PhPtCl_2$	**TU**	50 ± 3	43 ± 4	−105 ± 8	−142 ± 10
	DMTU	46 ± 3	44 ± 4	−129 ± 9	−165 ± 10
	TMTU	54 ± 1	52 ± 3	−155 ± 2	−176 ± 8
$CH_3PhPtCl_2$	**TU**	55 ± 2	45 ± 2	−129 ± 5	−151 ± 7
	DMTU	57 ± 2	48 ± 3	−156 ± 5	−174 ± 10
	TMTU	58 ± 2	53 ± 3	−189 ± 6	−186 ± 10
$CH_3OPhPtCl_2$	**TU**	53 ± 2	45 ± 3	−118 ± 9	−150 ± 9
	DMTU	56 ± 1	47 ± 3	−142 ± 3	−171 ± 9
	TMTU	57 ± 2	53 ± 4	−174 ± 6	−184 ± 11
$FPhPtCl_2$	**TU**	47 ± 1	40 ± 1	−95 ± 3	−120 ± 4
	DMTU	47 ± 1	44 ± 2	−121 ± 3	−156 ± 6
	TMTU	51 ± 1	49 ± 3	−146 ± 4	−164 ± 8

charges of $N_{1(py)}$ and $N_{2(amido)}$ or the bond lengths Pt–$N_{1(py)}$ and Pt–$N_{2(amido)}$ are significantly different. While both the pyridine and carboxamide ($CONH_2$/CONHR) donor groups of the ligand are electron-withdrawing, the former is a known strong π-acceptor of electron density from the non-bonding *d*-orbitals of the Pt-centers. The $CONH_2$/CONHR groups can only withdraw electron density from the metal centers by an inductive effect [36]. The trend in magnitude of the rate constants between the complexes is dependent on inductive effects. Through resonance of the coordinated amido groups, the electron density is easily delocalized from the Pt–$CONH_2$/CONHR bond into the molecular orbitals of the entire ligand. However, due to the stronger π-acceptor property and hence *trans* effect of pyridine in comparison to the amide, the Pt–Cl_1 bond length *trans* to it is marginally longer compared to the Pt–Cl_2 bond

length *trans* to the amido group. The nature of ancillary substituent on the amido nitrogen does not significantly influence the Pt–N and Pt–Cl bond lengths across all the complexes. The introduction of the phenyl group to the amide nitrogen for the rest of the complexes not only results in an increase in the Pt–N_2 bond length from **$PtCl_2$** to **$FPhPtCl_2$**, it also reduces the electronegativity of the nitrogen atom (N_2) due to the replacement of the strong σ-donor H-atom and reduces the charge on the Pt(II) metal center. The different ancillary substituents on the phenyl have limited electronic influence on the N_2 atom.

The electrophilicity index (ω) has been used as a structural-electron descriptor of the chemical reactivity of molecules [37–40]. A strong electrophile is characterized by a high value of ω [37]. The values in Table 2 show an increase of ω in the order **$PtCl_2$** (7.74) $>$ **$FPhPtCl_2$** (7.72) $>$ **$PhPtCl_2$** (7.34)$>$ **$CH_3PhPtCl_2$** (7.13) $>$ **$CH_3OPhPtCl_2$** (6.91) which agrees with the observed order of reactivity of the studied complexes except for **$CH_3PhPtCl_2$** and **$CH_3OPhPtCl_2$**. The same trend is observed for the relative values of Pt NBO charges (a representation of a point charge on the Pt atom) and the chemical potential (μ). From the above observation, one would expect **$CH_3OPhPtCl_2$** to be less reactive when compared to **$CH_3PhPtCl_2$**. However, from the data in Table 3, it is seen that **$CH_3PhPtCl_2$** is the least reactive because OCH_3 group withdraws electrons through an inductive effect.

The high reactivity of **$PtCl_2$** is also supported by the higher HOMO-LUMO energy gap (3.674 eV) (Figure 1) compared to the other complexes. This affirms that the complex is more reactive towards substitution of its labile ligand by incoming nucleophiles. In addition, its electronic chemical potential (μ), which relates to the capacity of the complex to exchange electron density with its immediate environment at the ground state [39], is the most negative. The strength of electron acceptor follows the order **$PtCl_2$** ($\mu = -5.334$) $>$ **$FPhPtCl_2$** ($\mu = -5.108$) $>$ **$PhPtCl_2$** ($\mu = -4.963$) $>$ **$CH_3PhPtCl_2$** ($\mu = -4.836$)=**$CH_3OPhPtCl2$** ($\mu = -4.691$) for the complexes studied.

The high rate of displacement of chlorides from **$PtCl_2$** (k_2 (1st)=347 ± 8; k_2 (2nd)=81 ± 2) when using **TU** as the nucleophile is due to strong electron withdrawing capacity of the unsubstituted carboxamide (–$CONH_2$) donor group. The presence of an electronegative carbonyl group causes the withdrawal of electrons from the nitrogen atom, making it electron deficient thereby enhancing its ability to withdraw electrons from the metal center. This is supported by the DFT data that show that the negative NBO charge on N_2 is much higher. This leads to an increase in removal of electrons from the metal center, thereby increasing the electrophilicity of the metal center and thus the reactivity of the complex towards the nucleophile.

The reactivity of **$PhPtCl_2$** (NH–phenyl) decreased by a factor of about 2.6 and 3 for the first and second substitution steps, respectively, compared to **$PtCl_2$**. The introduction of a phenyl group in **$PhPtCl_2$** changes the electronic properties of the complex. This is clearly supported by the changes in Pt–$N_{2(amido)}$ bond length, the NBO charge for N_2, the electronic chemical potential (μ) and the overall chemical electrophilicity (ω). The DFT optimized geometry of the complexes coordinated with ligands bearing a phenyl group, as indicated in Table 1 (last column), shows that the phenyl ring twists out of the coordination plane of the Pt(II) and the carboxamide ligand. According to the DFT data, the introduction of the –CH_3 or –OCH_3 as ancillary

substituent on the phenyl (–Ph) group does not however result in a significant change in electronic effect. However, the –FPh group increases the reactivity of **$FPhPtCl_2$** relative to **$PhPtCl_2$** due to its more electron-withdrawing ability in comparison to phenyl (–Ph) group. This is confirmed by an increase in ω and the total electrophilicity of the complex compared to **$PhPtCl_2$**. As already mentioned, all these trends are supported by trends in DFT-calculated parameters which reflects the geometrically optimized structures of the complexes. The DFT optimized geometry of the **$FPhPtCl_2$** illustrates that the phenyl ring (–FPh) is almost perpendicular to the coordination plane of Pt(II) and the carboxamide ligand. This observation explains the higher reactivity of **$FPhPtCl_2$** compared to all the complexes with the phenyl group (**$PhPtCl_2$**, **$CH_3OPhPtCl_2$** and **$CH_3PhPtCl_2$**).

The positive σ-inductive effect of the methyl or methoxy substituents at the *para*-position of the phenyl ring increases electron density of the phenyl ring and hence the carboxamide group coordinated to the metal. This reduces the electrophilicity of the metal centers for **$CH_3OPhPtCl_2$** and **$CH_3PhPtCl_2$**, thus reducing their reactivity compared to **$PhPtCl_2$**. **$CH_3OPhPtCl_2$** is more reactive when compared to **$CH_3PhPtCl_2$**, because the CH_3 in **$CH_3PhPtCl_2$** is an electron donor, whereas the OCH_3 withdraws electrons through an inductive effect.

In all complexes, the second substitution rate constants $k_{2(2nd)}$ are smaller than those for the first substitution $k_{2(1st)}$. The reduced reactivity for the second substitution step is attributed to the increase in steric hindrance caused by the first coordinated **TU**. The reactivity of the nucleophiles depends on steric effects, with the bulky **TMTU** being the least reactive. The negative entropy of activation for both substitution steps affirms an associative mode of substitution which is common for square-planar d^8 complexes.

Conclusion

Five bidentate Pt(II) complexes containing *N*-(4-substituted-phenyl)-(2-pyridine-carboxamide) chelating spectator ligands with varying substituents of different electronic properties were synthesized and characterized using different spectroscopic methods. The kinetics and mechanism of their substitution reactions with sulfur-donor nucleophiles were studied. Substitutions of two chloride leaving groups from the Pt(II) complexes were consecutive. The chloride co-ligand which is substituted first is one which is *trans* to the pyridine ring of the pyridyl-carboxamide ligand. The rate of consecutive chloride substitution from the complexes by the nucleophiles followed the order **$PtCl_2$** > **$FPhPtCl_2$** > **$PhPtCl_2$** > **$CH_3OPhPtCl_2$** > **$CH_3PhPtCl_2$**. The higher reactivity of **$PtCl_2$** is due to the stronger electro-polarizability of carbonyl group of the unsubstituted carboxamide which causes stronger withdrawal of electrons from the nitrogen atom, making the Pt center of the complex electron deficient and thus more reactive. The addition of an electron-donating phenyl group changes the electronic proportions of the complexes. The reactivity of the nucleophiles depends on steric effects, with the bulky **TMTU** being the least reactive. The consecutive chloride substitution steps are associatively activated given that the enthalpies of activation (ΔH_1 and ΔH_2) are low and positive while the entropies of activation (ΔS_1 and ΔS_2) are negative for both

substitution steps, which suggest an associative mode of activation for the substitution processes.

Acknowledgements

The authors gratefully acknowledge financial support from the University of KwaZulu-Natal and the National Research Foundation.

Disclosure statement

No potential conflict of interest was reported by the authors.

ORCID

Tshephiso R. Papo http://orcid.org/0000-0002-7860-1442
Deogratius Jaganyi http://orcid.org/0000-0003-4499-6877
Allen Mambanda http://orcid.org/0000-0002-8113-3643

References

[1] J. Reedijk. *Chem. Rev.*, **99**, 2499 (1999).
[2] V. Brabec, J. Kasparkova. *Drug Resist. Updat.*, **8**, 131 (2005).
[3] A.S. Abu-Surra, M. Kettunen. *Curr. Med. Chem.*, **13**, 1337 (2006).
[4] L. Kelland. *Nat. Rev. Cancer*, **7**, 573 (2007).
[5] M. Kantoury, M. Eslami-Moghadam, A.A. Tarlani, A. Divsalar. *Chem. Biol. Drug Des.*, **88**, 76 (2016).
[6] M.N. Patel, P.A. Dosi, B.S. Bhatt. *Acta Chim. Slov.*, **59**, 622 (2012).
[7] H. Mansouri-Torshizi, M. Eslami-Moghadam, A. Divsalar, A.A. Saboury. *Acta Chim. Slov.*, **58**, 811 (2011).
[8] M. Yodoshi, N. Okabe. *Chem. Pharm. Bull.*, **56**, 908 (2008).
[9] M.J. Rauterkus, S. Fakih, C. Mock, I. Puscasu, B. Krebs. *Inorg. Chim. Acta*, **350**, 355 (2003).
[10] J. Zhang, X. Ke, C. Tu, J. Lin, J. Ding, L. Lin, H.F. Fun, X. You, Z. Guo. *Biometals*, **16**, 485 (2003).
[11] Q. Lin, X. Lu, J. Chen, L. Li, X. He. *Spectrosc. Spect. Anal.*, **28**, 1359 (2008).
[12] L. Qiuyue, H. Xinqian, W. Donghang, Z. Jufang-Zhejiang, S.D. Xuebao. *Ziran Kexueban*, **32**, 189 (2009).
[13] A. Morsali, A. Ramazani, A.R. Mahjoub. *J. Coord. Chem.*, **56**, 1555 (2003).
[14] B.K. Signh, H.K. Rajour, R. Chauhan, S. Goyal. *Chem. Sci. Trans.*, **4**, 806 (2015).
[15] C.-Y. Shi, E.-J. Gao, S. Ma, M.-L. Wang, Q.-T. Liu. *Bioorg. Med. Chem. Lett.*, **20**, 7250 (2010).
[16] J.A. Fernandez-Poi, P.D. Hamilton, D.J. Klos. *Anticancer Res.*, **21**, 931 (2001).
[17] J.F. Holford, F.I. Raynaud, B.A. Murrer, K. Grimaldi, J.A. Hartley, M.J. Abrams, L.R. Kelland. *Anti-Cancer Drug Des.*, **13**, 1 (1998).
[18] D. Jaganyi, A. Hofmann, R. van Eldik. *Angew. Chem. Int. Ed.*, **40**, 1680 (2001).
[19] D. Jaganyi, D. Reddy, J.A. Gertenbach, A. Hofmann, R. van Eldik. *Dalton Trans.*, **2**, 299 (2004).
[20] A. Hofmann, D. Jaganyi, O.Q. Munro, G. Liehr, R. van Eldik. *Inorg. Chem.*, **42**, 1688 (2003).
[21] B.B. Khusi, A. Mambanda, D. Jaganyi. *Transit. Met. Chem.*, **41**, 191 (2016).
[22] G. Kinunda, D. Jaganyi. *Transit. Met. Chem.*, **41**, 235 (2016).
[23] W.M. Mthiyane, A. Mambanda, D. Jaganyi. *Transit. Met. Chem.*, **42**, 739 (2017).
[24] W.M. Mthiyane, A. Mambanda, D. Jaganyi. *Int. J. Chem. Kinet.*, **50**, 531 (2018).
[25] B.B. Khusi, A. Mambanda, D. Jaganyi. *J. Coord. Chem.*, **69**, 2121 (2016).

[26] D. Reddy, D. Jagany. *Dalton Trans.*, **6724**, 6724 (2008).
[27] J. Zhang, Q. Liu, C. Duan, Y. Shao, J. Ding, Z. Miao, X.-Z. You, Z. Guo. *J. Chem. Soc. Dalton Trans.*, 591 (2002).
[28] T. Mukherjee, S. Buddhadeb, E. Zangrando, G. Hundal, B. Chattopadhyay, P. Chattopadhyay. *Inorg. Chim. Acta*, **406**, 176 (2013).
[29] B. Miehlich, A. Savin, H. Stoll, H. Preuss. *Chem. Phys. Lett.*, **157**, 200 (1989).
[30] H.-M. Wen, Y.-H. Wu, Y. Fan, L.-Y. Zhang, C.-N. Chen, Z.-N. Chen. *Inorg. Chem.*, **49**, 2210 (2010).
[31] T. Shoeib, B.L. Sharp. *Metallomics*, **4**, 1308 (2012).
[32] B.A. Blight, S.-B. Ko, J. Lu, L.F. Smith, S. Wang. *Dalton Trans.*, **42**, 10089 (2013).
[33] G.W. Trucks, M.J. Frisch, H.B. Schlegel, G.E. Scuseria, J.R. Cheeseman, M.A. Robb, G. Scalmani, V. Barone, G.A. Petersson, B. Mennucci, H. Nakatsuji, M. Caricato, X. Li, A.F. Izmaylov, H.P. Hratchian, J. Bloino, G. Zheng, M. Hada, J.L. Sonnenberg, M. Ehara, K. Toyota, R. Fukuda, M. Ishida, J. Hasegawa, T. Nakajima, Y. Honda, O. Kitao, T. Vreven, H. Nakai, J.A. Montgomery Jr, J.E. Peralta, M. Bearpark, F. Ogliaro, J.J. Heyd, E. Brothers, K.N. Kudin, R. Kobayashi, V.N. Staroverov, J. Normand, K. Raghavachari, J. Rendell, S.S. Iyengar, J. Tomasi, M. Cossi, J. Rega, M. Klene, J.E. Knox, J.B. Cross, C. Adamo, V. Bakken, J. Jaramillo, R. Gomperts, R.E. Stratmann, O. Yazyev, A.J. Austin, R. Cammi, C. Pomelli, R.L. Martin, J.W. Ochterski, K. Morokuma, V.G. Zakrzewski, G.A. Voth, P. Salvador, J.J. Dannenberg, S. Dapprich, O. Farkas, A.D. Daniels, J.B. Foresman, J.V. Ortiz, J. Cioslowski, D.J. Fox. Gaussian 09 (Revision A. 1), Inc., Wallingford, CT (2009).
[34] J.R.L. Priqueler, I.S. Butler, F.D. Rochon. *Appl. Spectrosc. Rev.*, **41**, 185 (2006).
[35] J.D. Atwood. *Inorganic and Organic Reaction Mechanisms*, p. 32–34, 43–61, Wiley-VCH Inc., New York (1997).
[36] N. Summa, W. Schiessl, R. Puchta, N. van Eikema-Hommes, R. van Eldik. *Inorg. Chem.*, **45**, 2948 (2006).
[37] R.G. Pearson. *Acc. Chem. Res.*, **26**, 250 (1993).
[38] B. Semire, O.A. Odunola. *Int. J. Chem. Mod.*, **4**, 87 (2011).
[39] B. Semire. *Pakistan J. Sci. Ind. Res. A*, **56**, 14 (2013).
[40] L.R. Domingo, M. Ríos-Gutiérrez, P. Pérez. *Molecules*, **21**, 748 (2016).